Wang, K., & Richards, F. (1975) *J. Biol. Chem. 250*, 6622.
Weininger, M., Birktoft, J. J., & Banaszak, L. J. (1977) in *Pyridine Nucleotide-Dependent Dehydrogenases* (Sund, H., Ed.) pp 87–100, de Gruyter, New York.
Welch, G. R., Somogyi, B., & Damjanovich, S. (1982) *Prog. Biophys. Mol. Biol. 39*, 109.
Wilkinson, K. D., & Rose, I. R. (1980) *J. Biol. Chem. 255*, 7569.

Elementary Steps in the Reaction Mechanism of Chicken Liver Fatty Acid Synthase: Reduced Nicotinamide Adenine Dinucleotide Phosphate Binding and Formation and Reduction of Acetoacetyl-Enzyme†

Jean A. H. Cognet, Brian G. Cox,‡ and Gordon G. Hammes*

ABSTRACT: The kinetics of reduced nicotinamide adenine dinucleotide phosphate (NADPH) binding to fatty acid synthase from chicken liver and of the reduction of enzyme-bound acetoacetyl by NADPH (β-ketoacyl reductase) and the steps leading to formation of the acetoacetyl-enzyme have been studied in 0.1 M potassium phosphate–1 mM ethylenediaminetetraacetic acid (EDTA), pH 7.0, at 25 °C by monitoring changes in NADPH fluorescence with a stopped-flow apparatus. Improved fluorescence detection has permitted the use of NADPH concentrations as low as 20 nM. The kinetics of the binding of NADPH to the enzyme is consistent with a simple bimolecular binding mechanism and four equivalent sites on the enzyme (presumably two β-ketoacyl reductase sites and two enoyl reductase sites). The bimolecular rate constant is 12.7×10^6 M^{-1} s^{-1}, and the dissociation rate constant is 76.7 s^{-1}, which gives an equilibrium dissociation constant of 6.0 μM. The formation of the acetoacetyl-enzyme and its subsequent reduction by NADPH could be analyzed as two consecutive pseudo-first-order reactions by mixing enzyme–NADPH with acetyl-CoA and malonyl-CoA under conditions where [acetyl-CoA], [malonyl-CoA] >> [enzyme] >> [NADPH]. From the dependence of the rate of reduction of acetoacetyl-enzyme by NADPH on enzyme concentration, an independent estimate of the equilibrium dissociation constant for NADPH binding to the enzyme of 5.9 μM is obtained, and the rate constant for the reduction is 17.5 s^{-1}. The kinetic studies and analysis of the products obtained with [^{3}H]-NADPH suggest that the dehydration and enoyl reductase reactions occur much faster than the β-ketoacyl reductase reaction. The mechanism of formation of the acetoacetyl-enzyme is complex, but the inhibition of the rate of this process by high concentrations of both acetyl- and malonyl-CoA can be explained semiquantitatively in terms of a relatively rapid equilibration of these substrates with the enzyme followed by a rate-determining condensation reaction with a specific rate constant $\geq$30 s^{-1}. If CoA is scavenged from the reaction mixture, the rate of formation of the acetoacetyl-enzyme is greatly decreased; this indicates CoA is important for rapid formation of the acetoacetyl-enzyme. These results are consistent with those from steady-state kinetic studies.

The fatty acid synthase from chicken liver is a multienzyme complex containing two identical polypeptide chains of molecular weight 250000 (Yun & Hsu, 1972; Kumar et al., 1972; Arslanian et al., 1976; Stoops & Wakil, 1981). The enzyme catalyzes the synthesis of palmitic acid from AcCoA,[1] MalCoA, and NADPH through a series of reactions: after covalent transfer of malonyl and acetyl from MalCoA and AcCoA to the enzyme, malonyl and acetyl are condensed to form an acetoacetyl-enzyme intermediate; the enzyme-bound acetoacetyl is then reduced to hydroxybutyryl by NADPH; this is followed by dehydration to form crotonyl and a second reduction by NADPH to give enzyme-bound butyryl. This cycle is repeated 7 times by successive condensation of malonyl on to the growing hydrocarbon chain until palmitic acid is released by a thioesterase [cf. Bloch & Vance (1977)]. This mechanism is consistent with steady-state kinetic studies (Katiyar et al., 1975; Cox & Hammes, 1983) that have permitted an estimate of substrate binding constants and rate constants for the overall process. A systematic study of the individual steps in the reaction mechanism is being undertaken in our laboratory. A study of the acetylation and deacetylation of the enzyme by AcCoA and CoA, respectively, already has been reported (Cognet & Hammes, 1983). The rate constants for acetylation and deacetylation by enzyme-bound AcCoA and CoA are approximately 40 and 100 s^{-1}, respectively, at pH 7.0, 25 °C. In this work, the binding of NADPH to the enzyme, the reduction of enzyme-bound acetoacetyl by NADPH, and the formation of the acetoacetyl-enzyme from enzyme, AcCoA, and MalCoA have been studied with the stopped-flow method. Substrate dissociation constants and rate constants for individual steps in the mechanism have been obtained.

Materials and Methods

Materials. *N*-Acetyl-*S*-(acetoacetyl)cysteamine, 2,6-dichlorophenolindophenol, L-ascorbic acid, dithiothreitol, MalCoA, AcCoA, Mops, phosphotransacetylase, acetyl phosphate, and NADPH (type X) were from Sigma; ethyl butyrate, (*R*)-(−)-methyl 3-hydroxybutyrate, ethyl DL-2-

† From the Department of Chemistry, Cornell University, Ithaca, New York 14853. *Received June 28, 1983.* This work was supported by grants from the National Institutes of Health (GM 13292) and the National Science Foundation (PCM 8120818).

‡ Permanent address: Department of Chemistry, University of Stirling, Stirling, Scotland.

[1] Abbreviations: AcCoA, acetyl coenzyme A; MalCoA, malonyl coenzyme A; CoA, coenzyme A; EDTA, ethylenediaminetetraacetic acid; Mops, 3-(*N*-morpholino)propanesulfonic acid; NADPH, reduced nicotinamide adenine dinucleotide phosphate.

0006-2960/83/0422-6281$01.50/0

hydroxyvalerate, and hexanoyl chloride were from Aldrich; crotonyl chloride was from Eastman Kodak. Silica gel plates for thin-layer chromatography (80 × 40 mm with fluorescent indicator) were from Macherey-Nagel. All other chemicals were high-quality commercial grades, and all solutions were prepared with deionized, distilled water.

Fatty Acid Synthase. The enzyme was prepared from chicken liver as previously described (Cognet & Hammes, 1983). All experiments were carried out with enzyme in 0.1 M potassium phosphate–1 mM EDTA, pH 7.0, at 25 °C, except for one series of stopped-flow experiments where 0.1 M Mops was substituted for the potassium phosphate. The 10 mM dithiothreitol and 10% glycerol (w/v) necessary for storage of the purified enzyme were removed by passage through a 3-mL Sephadex G-50 fine centrifuge column (Penefsky, 1977). The specific activity of the enzyme, measured under standard conditions (Cardon & Hammes, 1982), was 1.6 μmol of NADPH/(mg·min). The protein concentration was determined by measurement of the absorbance at 280 nm, with an extinction coefficient for fatty acid synthase of 4.82 × 10^5 M^{-1} cm^{-1} (Hsu & Yun, 1970).

Stopped-Flow Measurements. The stopped-flow experiments were performed on a modified (Akiyama & Hammes, 1981) Durrum-Gibson stopped-flow spectrophotometer (Dionex Corp.) thermostated at 25 °C. The light source was a 200-W xenon–mercury arc lamp (Conrad-Hanovia). The dead time of the instrument was found to be 1–3 ms by use of two standard reactions, the reduction of 2,6-dichlorophenolindophenol by ascorbic acid (absorbance mode) and the binding of 8-anilino-1-naphthalenesulfonic acid to bovine serum albumin (fluorescence mode). The sensitivity of detection in the fluorescence mode was greatly enhanced by the use of a half-mirrored observation cell that was placed in an aluminum cavity. The cavity served as a light collector and extended directly into the photomultiplier housing. A 2-mm ultraviolet cut-off filter (37% transmittance at 420 nm; Corning 3389) was inserted in front of the photomultiplier tube inside the housing. The photomultiplier housing was positioned as close as possible to the observation cell, and a light-tight seal to the aluminum light collector was made with an O ring. The fluorescence of NADPH was monitored with an excitation wavelength of 367 nm. Fluorescence changes could be detected with initial NADPH concentrations as low as 20 nM.

In a typical stopped-flow experiment, 0.14 mL of each of the reactants was mixed. Control experiments indicated the enzyme was not denatured by passage through the stopped-flow apparatus, which was periodically washed with methanol–KOH. The kinetic data were transferred through a transient recorder (Biomation 802) to a PDP 11/24 computer (Digital Equipment Corp.) for processing and storage. Data were fit to specified equations by a least-squares analysis.

Product Analysis. The enzyme (final concentration 1.1 μM) was rapidly mixed with AcCoA, MalCoA (60 and 30 or 70 and 140 μM), and tritiated NADPH (a generous gift of Dr. V. E. Anderson; final concentration 0.3–1.6 μM) specifically labeled at the *pro*-4*R* (800 cpm/pmol) or *pro*-4*S* (1500 cpm/pmol) position in a quenched-flow apparatus at 25 °C. After 5–10 s, 80 μL of neutralized hydroxylamine (~2 M) was added to 400 μL of the reaction mixture and incubated 10 or 60 min. The enzyme then was precipitated by shaking after addition of a few drops of concentrated HCl and chloroform.

A few microliters of the supernatant was spotted on silica gel thin-layer chromatography plates that were developed in ether–glacial acetic acid (96:4). Standard compounds were detected on the chromatographic plates by observation of fluorescence excited with light at 254 nm and by spraying the plate with concentrated ferric chloride (0.5 M). The products were detected by cutting the plate into strips and by incubating the strips with 10 mL of aqueous counting scintillant (Amersham) for at least 24 h before determining the radioactivity with a Beckman LS-255 scintillation counter. Various synthesized hydroxamic acids were used as standards. The hydroxamic acids of butyrate, 3-hydroxybutyrate, and DL-2-hydroxyvalerate were prepared from their esters by reacting 0.005 mol of the methyl or ethyl ester with 0.01 mol of hydroxylamine hydrochloride and 1.5 g of sodium hydroxide in 5 mL of distilled deionized water for 4 min at 100 °C. The hydroxamic acids of crotonyl and hexanoyl were prepared from crotonyl chloride and hexanoyl chloride by reacting 0.005 mol of the chloride with 0.05 mol of hydroxylamine hydrochloride and 2.8 g of sodium hydroxide dissolved in 8 mL of distilled deionized water for 10 min at 0 °C. The reaction mixture was agitated to ensure reaction between the two layers, and the pH of the solution then was adjusted to 5–6 with concentrated HCl. The hydroxamic acids of crotonyl and hexanoyl were extracted with ether and redissolved in the standard buffer for spotting on chromatography plates. The hydroxamic acid of acetoacetate was prepared by reacting 250 μL of 0.76 M *N*-acetyl-*S*-(acetoacetyl)cysteamine in the standard buffer with 50 μL of 2.0 M neutralized hydroxylamine for 10 min at room temperature.

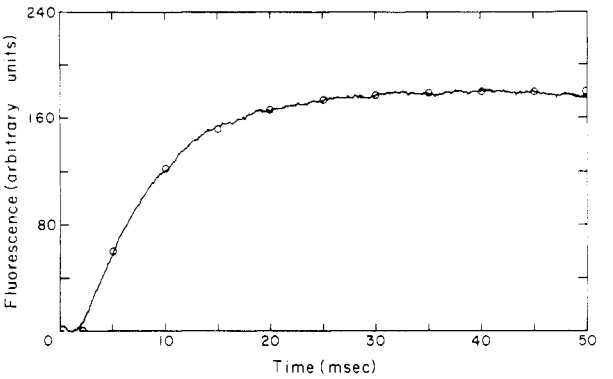

FIGURE 1: A typical stopped-flow kinetic trace of change in fluorescence following mixing of enzyme (final concentration 0.20 μM) and NADPH (final concentration 11.7 μM) in 0.1 M potassium phosphate–1 mM EDTA, pH 7.0 at 25 °C. The open circles have been calculated with eq 1 and the best fit parameters $F(\infty) = 180$, $A = -245$, and $k_{obsd} = 144$ s^{-1}. The complete calculated curve is virtually coincidental with the kinetic trace.

Results

Binding of NADPH to Enzyme. If NADPH is mixed with enzyme in the stopped-flow apparatus at 25 °C in 0.1 M potassium phosphate–1 mM EDTA, pH 7.0, an enhancement in fluorescence occurs. A typical kinetic trace is shown in Figure 1. The time course can be fit to the first-order rate equation

$$F(t) - F(\infty) = A \exp(-k_{obsd}t) \quad (1)$$

over a range of NADPH (0.02–29.2 μM) and enzyme (0.18–1.63 μM) concentrations. In eq 1, $F(t)$ is the fluorescence at time t, A is a constant, and k_{obsd} is a first-order rate constant. The open circles in Figure 1 have been calculated with eq 1; the complete calculated curve is virtually coincidental with the experimental trace. If the simple bimolecular binding mechanism

$$E + NADPH \underset{k_r}{\overset{k_f}{\rightleftharpoons}} E{\cdot}NADPH$$

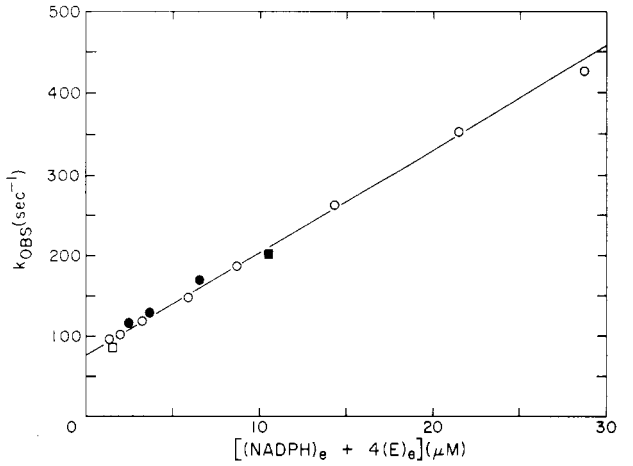

FIGURE 2: Plot of observed first-order rate constant for binding of NADPH to enzyme, k_{obsd} vs. sum of equilibrium concentrations of unbound NADPH and unoccupied NADPH binding sites on the enzyme, $[NADPH]_e + 4[E]_e$. Each point is the average of at least three kinetic experiments. For the open circles, the final total enzyme concentration was 0.20 μM, while for the filled circles the molar ratio of the total enzyme to NADPH was 8.5. The squares indicate experiments in which the rate of dissociation of the enzyme was measured with either excess NADPH (open) or excess enzyme (filled). Other experimental conditions were as in the legend to Figure 1.

is assumed, the observed first-order rate constant near equilibrium is

$$k_{obsd} = k_f([NADPH]_e + n[E]_e) + k_r \quad (2)$$

Here k_f is the bimolecular rate constant for formation of the complex, k_r is the dissociation rate constant, n is the number of equivalent NADPH binding sites on the enzyme, and the subscript e denotes the equilibrium concentrations. The value of n was determined by studying the reaction under two limiting (pseudo-first-order) conditions: $[NADPH]_e >> [E]_e$ and $[E]_e >> [NADPH]_e$. In the former case, a plot of k_{obsd} vs. [NADPH] is a straight line with a slope of $k_f = 12.5 \times 10^6$ M^{-1} s^{-1}. In these experiments, [NADPH] = 5–29 μM, and the total enzyme concentration was 0.2 μM. In the latter case, a plot of k_{obsd} vs. [E] is a straight line with a slope of $nk_f = 53.2 \times 10^6$ M^{-1} s^{-1}. In these experiments, the concentration of enzyme (0.18–1.63 μM) was 8.5 times that of NADPH. These results indicate that $n = 4$. The values of k_{obsd} were then fit to eq 2 over the entire range of concentrations employed. The equilibrium concentrations were obtained by successive approximations: an equilibrium constant was assumed, and the rate constants obtained from the kinetic analysis were used to calculate a new equilibrium constant; this procedure was continued until the assumed equilibrium constant was equal to that obtained from the kinetic analysis. The data are summarized in Figure 2 as a plot of k_{obsd} vs. $[NADPH]_e + n[E]_e$. Filled circles indicate that $[E]_e >> [NADPH]_e$. Linear regression analysis of this plot with a constant percent error weighting gives $k_f = 12.7$ ($\pm$0.5) $\times 10^6$ M^{-1} s^{-1}, $k_r = 76.7$ ($\pm$2.8) s^{-1}, and $K_d = k_r/k_f = 6.0$ μM. The line in Figure 2 has been calculated with these parameters and eq 2. Also included in Figure 2 are two values of k_{obsd} obtained by observing the dissociation of NADPH from the enzyme following the mixing of enzyme–NADPH solutions with buffer. In all cases, no significant deviation from first-order behavior was observed in the time course of the reaction.

NADPH Oxidation by β-Ketoacyl Reductase. The first oxidation of NADPH in the reaction sequence catalyzed by fatty acid synthase occurs when acetoacetyl is reduced by NADPH. The study of this step in the reaction sequence requires careful design of the experiment if readily interpretable results are to be obtained. If the experiment is done under the conditions normally employed with enzymes, namely a high concentration of substrates relative to enzyme, many turnovers occur, and the kinetic traces are complex. The simplest method of limiting the number of turnovers is to use a high concentration of enzyme relative to NADPH. The rate of oxidation of NADPH then will be pseudo first order since the concentration of the enzyme species being reduced remains essentially constant throughout the course of the reaction. Generation of the acetoacetyl-enzyme intermediate that is reduced also can be made pseudo first order if the concentration of enzyme reacted with the substrates AcCoA and MalCoA is much less than the concentrations of these substrates. If the generation of the acetoacetyl intermediate, EAcac, is assumed to be characterized by a single first-order rate constant k_1, then

$$[EAcac] = [E_0](1 - e^{-k_1 t}) \quad (3)$$

where $[E_0]$ is the total enzyme concentration and k_1 is a function of the AcCoA and MalCoA concentrations. The reduction of EAcac to hydroxybutyryl-enzyme can be described by the rate equation

$$-\frac{d[NADPH]}{dt} = k_{2s}[NADPH][EAcac] \quad (4)$$

where [NADPH] represents the total concentration of reduced nucleotides and k_{2s} is a second-order rate constant. Since $[E_0] >> [NADPH]$, eq 4 can be combined with eq 3 and rewritten as

$$-\frac{d[NADPH]}{dt} = k_{2s}[E_0](1 - e^{-k_1 t})[NADPH] \quad (5)$$

Integration of eq 5 gives

$$[NADPH] = [NADPH]_0 \exp(-k_2[t + (1/k_1)(e^{-k_1 t} - 1)]) \quad (6)$$

where $[NADPH]_0$ is the concentration of NADPH at $t = 0$ and $k_2 = k_{2s}[E_0]$. This simple formulation does not take into account that half of the bound NADPH is at enoyl reductase sites and that further reduction of hydroxybutyryl-enzyme (after dehydration) can occur at these sites. However, as documented below, the reduction of hydroxybutyryl is much more rapid than the reduction of acetoacetyl, and therefore, the formulation above is correct. The factor of 2 in the rate law due to a second NADPH disappearing for each acetoacetyl reduced is cancelled by the fact that only half of the NADPH is bound at β-ketoacyl reductase sites. If $k_1 >> k_2$, eq 6 predicts that a brief lag period (characterized by k_1) will occur while the enzyme is converted to EAcac; this is followed by a first-order decay of the NADPH concentration characterized by k_2.

In the actual experiments, the enzyme was premixed with NADPH to minimize the fluorescence changes associated with the NADPH–enzyme binding reaction, which is rapid compared with the rate of formation of EAcac and the oxidation of NADPH. The NADPH–enzyme mixture was then mixed with AcCoA and MalCoA (56 and 98 μM, respectively, after mixing) in the stopped-flow apparatus at 25 °C in the standard buffer. The molar ratio [enzyme]/[NADPH] was kept constant at 2.85, with the concentration of enzyme varying from 0.118–2.14 μM. (Note that the molar ratio of NADPH binding sites to NADPH is ~11.) A typical kinetic trace is shown in Figure 3. The data conform to eq 6 very precisely with $[NADPH] = F(t) - F(\infty)$ and $[NADPH]_0 = A$ = constant; the open circles in Figure 3 have been calculated with

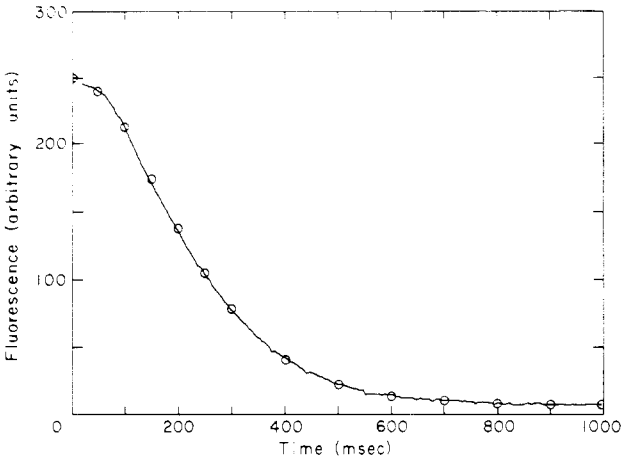

FIGURE 3: A typical stopped-flow kinetic trace of change in fluorescence following mixing of enzyme (2.14 μM)–NADPH (0.75 μM) with AcCoA (56 μM) and MalCoA (98 μM) in 0.1 M potassium phosphate buffer–1 mM EDTA, pH 7.0 at 25 °C. (All concentrations are after mixing.) The open circles have been calculated with the best fit parameters k_1 = 4.3 s^{-1}, k_2 = 9.5 s^{-1}, A = 244, and $F(\infty)$ = 7.2, according to eq 6 and the relationships [NADPH] = $F(t) - F(\infty)$ and $[NADPH]_0 = A$. The complete calculated curve is virtually coincidental with the kinetic trace.

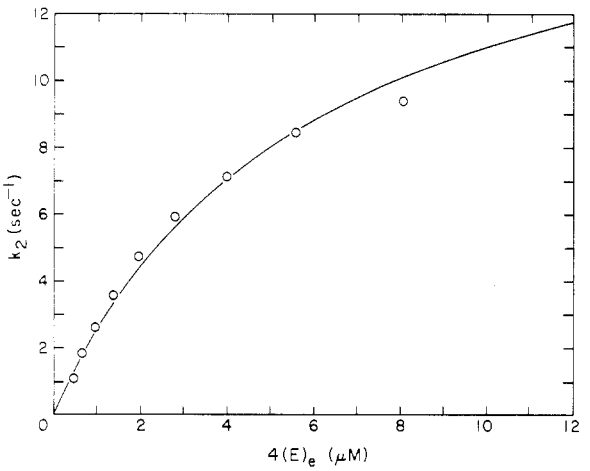

FIGURE 4: Plot of pseudo-first-order rate constant for oxidation of NADPH by fatty acid synthase, k_2, vs. equilibrium concentration of unoccupied NADPH sites, 4[E]$_e$. The molar ratio of total enzyme to total NADPH is constant (2.85) for all points. The other experimental conditions are the same as in the legend to Figure 3. The curve was calculated with eq 8 and the best fit parameters k_2' = 17.5 s^{-1} and K_d = 5.9 μM, assuming a constant percent error weighting.

eq 6 and the best fit parameters. The complete curve is virtually coincidental with the experimental trace. The value of k_1 varied slightly as the concentrations of enzyme and NADPH were varied. In order to eliminate any covariance of k_1 and k_2, the data were reanalyzed with k_1 fixed at its average value, 4.3 s^{-1}. The values of k_2 obtained as a function of the equilibrium concentration of empty NADPH binding sites, 4[E]$_e$, are shown in Figure 4. These data suggest the reduction mechanism consists of a rapid binding of NADPH followed by relatively slow reduction:

$$\text{EAcac} + \text{NADPH} \overset{K_d}{\rightleftharpoons} \text{EAcac·NADPH} \xrightarrow{k_2'} \text{E-hydroxybutyryl} + \text{NADP}^+ \quad (7)$$

For this mechanism

$$k_2 = \frac{k_2'}{1 + K_d/(4[E]_e)} \quad (8)$$

Analysis of the results in Figure 4 according to eq 8 gives k_2' = 17.5 (±2.6) s^{-1} and K_d = 5.9 (±1.2) μM if a constant percent error weighting is assumed. [For constant absolute error weighting, k_2' = 14.6 (±0.7) s^{-1} and K_d = 4.2 (±0.4) μM.] An iterative method similar to that used in fitting data to eq 2 was used to obtain [E]$_e$. The curve in Figure 4 has been calculated with the first set of parameters and eq 8.

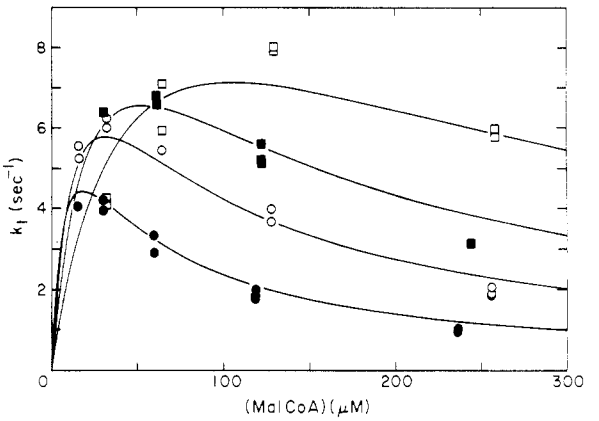

FIGURE 5: Plot of pseudo-first-order rate constant for formation of acetoacetylated enzyme, k_1, vs. concentration of MalCoA at AcCoA concentrations of 234 (□), 108 (■), 57.6 (○), and 26.0 (●) μM. The concentrations of enzyme and NADPH were 2.0 and 0.35 μM, respectively. Other experimental conditions are the same as in the legend to Figure 3. The curves were calculated with eq 10 and the best fit parameters K_A = 19.2 μM, K_M = 8.0 μM, and k_3 = 30.9 s^{-1}. A constant absolute error weighting was used in fitting the data.

The dependence of k_1 on the concentrations of AcCoA (26.0–234 μM) and MalCoA (15.0–258 μM) was studied at constant concentrations of enzyme (2.0 μM) and NADPH (0.35 μM). In fitting the time-course data, the value of k_2 was kept fixed at 9.1 s^{-1}, which was the average value (±1.0) obtained from 34 kinetic traces fit to eq 6. The dependence of k_1 on the concentrations of AcCoA and MalCoA is shown in Figure 5. A simple mechanism reasonably consistent with the data assumes rapid formation of the acetyl- and malonyl-enzyme followed by a relatively slow condensation reaction. This mechanism can be written as

$$\text{E} + \text{AcCoA} \overset{K_A}{\rightleftharpoons} \text{EAc} + \text{CoA}$$

$$\text{E} + \text{MalCoA} \overset{K_M}{\rightleftharpoons} \text{EMal} + \text{CoA}$$

$$\text{EAc} + \text{MalCoA} \overset{K_M}{\rightleftharpoons} \text{EAcMal} + \text{CoA} \xrightarrow{k_3} \text{EAcac} + \text{CoA}$$

$$\text{EMal} + \text{AcCoA} \overset{K_A}{\rightleftharpoons} \text{EAcMal} + \text{CoA} \xrightarrow{k_3} \text{EAcac} + \text{CoA} \quad (9)$$

In addition, the results in Figure 5 indicate that both AcCoA and MalCoA act as inhibitors. MalCoA is approximately twice as effective as an inhibitor and as a substrate. If this is assumed to be simple competitive inhibition characterized by the dissociation constants K_A and K_M

$$k_1 = k_3[\text{AcCoA}][\text{MalCoA}]/\{[[\text{AcCoA}] + K_A(1 + [\text{MalCoA}]/K_M)][[\text{MalCoA}] + K_M(1 + [\text{AcCoA}]/K_A)]\} \quad (10)$$

The curves in Figure 5 represent the best fit to eq 10 with k_3 = 30.9 (±0.9) s^{-1}, K_A = 19.2 (±2.7) μM, and K_M = 8.0 (±1.0) μM. [A constant absolute error weighting was assumed in the data analysis since the experimentally determined rate constant is more precise near the maxima in Figure 5.] Some data also were obtained at lower concentrations of AcCoA (<26 μM) and MalCoA (<15 μM) but were not used in the data analysis because the substrate concentrations were comparable to the

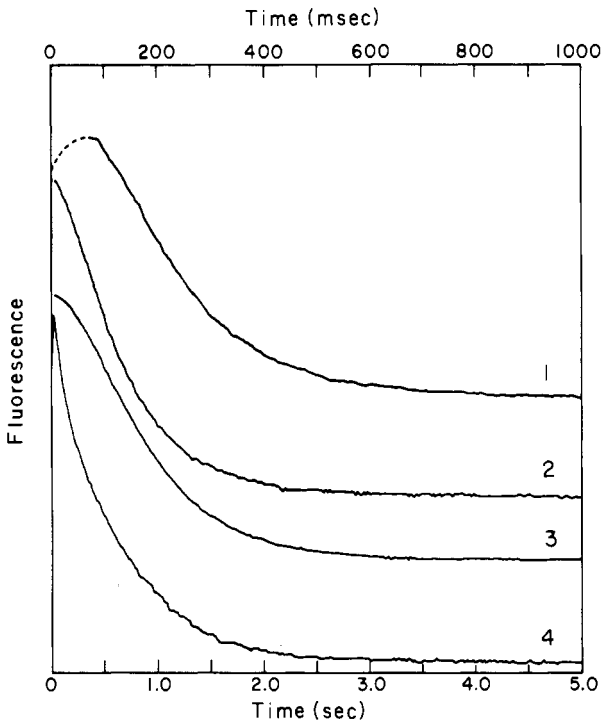

FIGURE 6: Typical stopped-flow kinetic traces of change in fluorescence vs. time. (1) 3.94 μM enzyme and 0.7 μM NADPH were mixed with 200 μM AcCoA and 100 μM MalCoA. (The dashed line was not used in the data fitting.) (2) 3.94 μM enzyme, 0.7 μM NADPH, and 200 μM AcCoA (incubated for a few minutes) were mixed with 100 μM MalCoA. (3) 3.94 μM enzyme, 0.7 μM NADPH, and 100 μM MalCoA (incubated for 3 min) were mixed with 200 μM AcCoA. (4) 3.94 μM enzyme, 200 μM AcCoA, 10 mM acetyl phosphate, and ~200 units/mL phosphotransacetylase (incubated for 3–62 min) were mixed with 100 μM MalCoA and 0.7 μM NADPH. The top time scale applies to the upper three traces and the bottom time scale to the lower trace. All experiments were in 0.1 M Mops–1 mM EDTA, pH 7.0 at 25 °C.

enzyme concentration, thereby making the assumption of pseudo first order invalid. These data also qualitatively conform to the postulated mechanism.

A set of stopped-flow experiments also was carried out to study the effect of incubating the enzyme with AcCoA and MalCoA prior to mixing with NADPH and the effect of scavenging CoA from the incubation mixture with phosphotransacetylase and acetyl phosphate. In these experiments, 0.1 M Mops was substituted for the potassium phosphate, which is a substrate of phosphotransacetylase. The top curve in Figure 6 is a control experiment in which 3.94 μM enzyme and 0.7 μM NADPH were mixed with 200 μM AcCoA and 100 μM MalCoA. The dashed line is due to a relatively slow reaction of NADPH with the enzyme in Mops and was not used in the data fitting; the remainder of the curve is coincidental with the theoretical curve calculated with eq 6 and the best fit parameters $k_1 = 4.9\ s^{-1}$ and $k_2 = 8.7\ s^{-1}$. (In phosphate buffer under comparable conditions, $k_1 = 6.5\ s^{-1}$ and $k_2 = 9.1\ s^{-1}$.) The second trace was obtained when AcCoA and NADPH were incubated with the enzyme for a few minutes prior to mixing with MalCoA. The slow reaction of NADPH with the enzyme does not occur in this case, and $k_1 = 22\ s^{-1}$ and $k_2 = 9.4\ s^{-1}$. If MalCoA and NADPH are incubated with the enzyme for 3 min prior to mixing with AcCoA (trace 3), $k_1 = 9.7\ s^{-1}$ and $k_2 = 8.7\ s^{-1}$. For this experiment, the MalCoA was purified by high-performance liquid chromatography (Cox & Hammes, 1983). For both traces 2 and 3, the calculated curves are coincidental with the experimental trace. As expected, if MalCoA is incubated with the enzyme for long times (>15 min), the enzyme is significantly inhibited (Kumar & Srinivasan, 1981). If the enzyme is incubated with AcCoA, 10 mM acetyl phosphate, and about 200 units/mL of phosphotransacetylase for 3–62 min and mixed with 100 μM MalCoA and 0.7 μM NADPH, trace 4 is obtained. No lag period is observed, and the curve can be fit approximately by a single exponential decay. If the sum of two exponential decays is assumed, the trace and calculated curves are coincidental. The smaller first-order rate constant, which accounts for 82% of the amplitude, is 1.6 s^{-1}. (The larger first-order rate constant is 17 s^{-1}.) Since 1.6 s^{-1} is significantly smaller than the measured rate constant for reduction of the acetoacetyl-enzyme (8.7 s^{-1}), formation of the acetoacetyl-enzyme has become rate determining for at least 82% of the overall reaction and is substantially slower than that in the control experiment (4.9 s^{-1}). Therefore, the presence of CoA significantly increases the observed rate of formation of the acetoacetyl-enzyme. Similar experiments were carried out with MalCoA preincubated with the enzyme, phosphotransacetylase, and acetyl phosphate prior to mixing with NADPH and AcCoA. In this case, the results obtained depend on the time of incubation. Again, the trace does not show a lag period, and the sum of two exponential decays is required to fit the data. However, the rate constants and relative amplitudes of the two exponentials are dependent on the time of incubation. At short incubation times (<2 min), the two rate constants are about 13 s^{-1} and 3 s^{-1} with relative amplitudes of $^2/_3$ and $^1/_3$.

Table I: Product Analysis of Reaction of Fatty Acid Synthase-[^{3}H]NADPH with AcCoA and MalCoA[a]

R_f	origin	0.02	0.2–0.35	0.35–0.45	0.45–0.55	0.55–0.68
% counts	18 ± 4	7 ± 3	9 ± 3	50 ± 4	7 ± 1	5 ± 1

[a] Summary of four experiments.

Product Analysis. The R_f values for the authentic samples are as follows: 3-hydroxbutyrate, 0.15–0.19; acetoacetate, 0.31; DL-hydroxyvalerate, 0.46; butyrate, 0.53; crotonate, 0.57; hexanoate, 0.60. All of the samples were the hydroxamic acid derivatives of the above. The results of four experiments are summarized in Table I. Analysis of [^{3}H]NADPH in a separate control experiment in the same chromatographic system indicates that >94% stays at the origin. The peak in product radioactivity (61% of the counts not at the origin) has an R_f value of 0.35–0.45, which clearly is not hydroxybutyryl or crotonyl (the first reduction products) or butyryl (the second reduction product). The product probably corresponds to the keto acid produced by reaction of tritiated butyrate with malonyl-enzyme (β-ketohexanoic acid). This interpretation is consistent with the following facts: the peak has a slightly larger R_f value than acetoacetate, as expected for a β-keto acid with a larger hydrocarbon chain, and the same results were obtained with *pro*-4*R*- or *pro*-4*S*-tritiated NADPH. The β-ketoacyl reductase stereospecifically utilizes the *pro*-4*S* hydrogen and the enoyl reductase the *pro*-4*R* hydrogen (V. E. Anderson and G. G. Hammes, unpublished results). The product analysis, therefore, indicates the enoyl reductase reaction is much faster than the β-ketoacyl reductase reaction.

Discussion

Three reactions associated with the catalytic action of fatty acid synthase have been studied: the binding of NADPH by the enzyme, the reduction of enzyme-bound acetoacetyl by NADPH (β-ketoacyl reductase), and the condensation of enzyme-bound acetyl and malonyl (β-ketoacyl synthase). The binding reaction is well behaved and indicates four independent sites on the enzyme for NADPH with essentially identical

dissociation constants, ~6 μM. Presumably, two of these are associated with β-ketoacyl reductase and two with enoyl reductase. The finding of four equivalent binding sites is in agreement with previous work that used fluorescence titrations and forced dialysis (Cardon & Hammes, 1982; Hsu & Wagner, 1970). However, the dissociation constants obtained from the equilibrium binding measurements were considerably smaller (<1 μM). No explanation for this discrepancy has been found. The kinetic results of this work are consistent with steady-state studies that place a lower bound of ~3 μM on the dissociation constant (Cox & Hammes, 1983). Some evidence for nonequivalent binding sites has been reported (Srinivasan & Kumar, 1976) but was not found in our kinetic studies.

The dissociation constant for NADPH binding to the β-ketoacyl reductase sites obtained from the study of the reduction of enzyme-bound acetoacetyl by NADPH of ~5.9 μM is in good agreement with the value obtained from the kinetic study of the binding of NADPH to the enzyme. The technique of making the reaction of AcCoA and MalCoA with the enzyme first order with respect to enzyme (high substrate concentrations relative to enzyme) and the subsequent reduction first order with respect to NADPH (high enzyme concentration relative to NADPH) was crucial in obtaining results that could be quantitatively analyzed. Both the product analysis and the kinetics are consistent with the β-ketoacyl reductase enzyme having a much smaller turnover number than that of the enoyl reductase. This is not unexpected since the standard free-energy change for the conversion of crotonyl-CoA to butyryl-CoA by NADPH is considerably more favorable than that for the conversion of acetoacetyl-CoA to β-hydroxybutyryl-CoA (−60 kJ vs. −17 kJ; Metzler, 1977).

An analysis of the pseudo-first-order rate constant characterizing the reaction of the enzyme with AcCoA and MalCoA to form acetoacetyl-enzyme is complex, and the treatment given in this work can only be considered approximate. This is because the condensation reaction may not be overwhelmingly rate determining; at low concentrations of MalCoA and/or AcCoA, the rate of the acyl-transfer reactions must also be of importance. However, the dependence of the rate constant on the concentrations of AcCoA and MalCoA is semiquantitatively consistent with the condensation reaction being rate determining. The concentration dependence of the rate constant is inconsistent with either acyl-transfer reaction being rate determining over the whole range of substrate concentrations. The dissociation constants for AcCoA (19 μM) and MalCoA (8 μM) are greater than the steady-state Michaelis constants (0.72 and 2.5 μM, respectively; Cox & Hammes, 1983), which are lower bounds to the actual dissociation constants. However, some CoA is present in the stopped-flow experiments, which probably causes the measured dissociation constants to be larger than the true constants. The steady-state inhibition constants are also much less than the dissociation constants, and AcCoA inhibits the steady-state reaction about twice as effectively as MalCoA, whereas the converse is true in the results reported here. However, this is not unexpected as the inhibition of the steady-state reaction, where seven MalCoA molecules are utilized for each AcCoA, is a quite different process than the 1:1 condensation reaction.

The rate of acetylation of the enzyme by enzyme-bound AcCoA has been found to be ~40 s^{-1}; the dissociation constant for AcCoA binding to the enzyme was estimated to be 20–80 μM (Cognet & Hammes, 1983), in fair agreement with the estimate obtained in this work for a somewhat different process. The rate constant for acetylation is not much greater than that for condensation and may be partially rate determining at low concentrations of AcCoA and/or high concentrations of MalCoA. The data do not justify inclusion of this additional complication into the mechanism. However, the qualitative consequence of this would be to make the observed first-order rate constant for the condensation a lower bound to the true rate constant. The contribution of the acetylation, condensation, and β-ketoacyl reductase reactions to the steady-state turnover number is $(^1/_{40} + ^7/_{30} + ^7/_{17})^{-1}$ = 1.5 s^{-1} if all of the steps in the synthesis of palmitic acid are assumed to be independent of fatty acid chain length. This is approximately twice as large as the observed turnover number, 0.8 s^{-1} (Cox & Hammes, 1983). Thus other reactions in the catalytic cycle must make a significant contribution to the turnover number.

The experiments in which AcCoA or MalCoA are incubated with the enzyme prior to initiating the reaction give some insight into the nature of the rate-determining step for the formation of the acetoacetyl-enzyme. Preincubation with AcCoA increases k_1 from 4.9 to 22 s^{-1}, indicating the acetylation process is contributing significantly to k_1 at low concentrations of AcCoA, although the extrapolated condensation rate constant of 30 s^{-1} is not reached. Preincubation with MalCoA increases k_1 from 4.9 to 9.7 s^{-1}, which is a relatively small increase. Since prior formation of the malonylated enzyme does not increase k_1 nearly as much as prior formation of the acetylated enzyme, malonylation is not significantly rate determining in the formation of the acetoacetyl-enzyme under the experimental conditions employed. In both of the above experiments, the rate constant characterizing the oxidation of NADPH is essentially unchanged. However, when CoA is scavenged from the AcCoA–enzyme system, the acetyl groups apparently are locked in the wrong position on the enzyme so that the uptake of MalCoA is inhibited: the lag period is not observed, and a relatively slow rate of NADPH oxidation occurs. The small fraction of rapidly reacting enzyme can be attributed to some of the malonyl sites still being accessible and/or the phosphotransacetylase not being 100% efficient. Preincubation of MalCoA-enzyme with phosphotransacetylase does not produce such a dramatic effect, although a substantial fraction of the MalCoA-enzyme mixture reacts slowly with NADPH. This experiment is flawed by the fact that AcCoA is produced by phosphotransacetylase during the incubation and by the complex interactions of MalCoA with the enzyme (Kumar & Srinivasan, 1981). However, malonyl groups do not appear to block the formation of acetoacetyl by the enzyme as effectively as acetyl groups. In any event, these results indicate the presence of CoA significantly increases the rate of formation of the acetoacetyl-enzyme, presumably by allowing malonyl and acetyl groups to equilibrate rapidly with the enzyme until the correct configuration of acetyl and malonyl groups on the enzyme is attained. A similar conclusion has been reached by others on the basis of different experiments (Stern et al., 1982; Soulié et al., 1983).

Studies to obtain additional information about the kinetics of the individual steps in the reaction sequence catalyzed by fatty acid synthase are continuing.

Registry No. Fatty acid synthase, 9045-77-6; β-ketoacyl reductase, 37250-34-3; enoyl reductase, 37251-09-5; NADPH, 53-57-6; AcCoA, 72-89-9; MalCoA, 524-14-1; β-ketohexanoic acid, 4380-91-0.

References

Akiyama, S. K., & Hammes, G. G. (1981) *Biochemistry 20*, 1491–1497.

Arslanian, M. J., Stoops, J. K., Oh, Y. H., & Wakil, S. J. (1976) *J. Biol. Chem. 251*, 3194–3196.

Bloch, K., & Vance, D. (1977) *Annu. Rev. Biochem. 46*, 263–298.
Cardon, J. W., & Hammes, G. G. (1982) *Biochemistry 21*, 2863–2870.
Cognet, J. A. H., & Hammes, G. G. (1983) *Biochemistry 22*, 3002–3007.
Cox, B. G., & Hammes, G. G. (1983) *Proc. Natl. Acad. Sci. U.S.A. 80*, 4233–4237.
Hsu, R. Y., & Wagner, B. J. (1970) *Biochemistry 9*, 245–251.
Hsu, R. Y., & Yun, S. L. (1970) *Biochemistry 9*, 239–245.
Katiyar, S. S., Cleland, W. W., & Porter, J. W. (1975) *J. Biol. Chem. 250*, 2709–2717.
Kumar, S., & Srinivasan, K. R. (1981) *Biochemistry 20*, 3393–3400.
Kumar, S., Muesing, R. A., & Porter, J. W. (1972) *J. Biol. Chem. 247*, 4749–4762.
Metzler, D. E. (1977) *Biochemistry: The Chemical Reactions of Living Cells*, p 173, Academic Press, New York.
Penefsky, H. S. (1977) *J. Biol. Chem. 252*, 2891–2899.
Soulié, J. M., Sheplock, G. J., Tian, W., & Hsu, R. Y. (1983) *J. Biol. Chem.* (in press).
Srinivasan, K. R., & Kumar, S. (1976) *J. Biol. Chem. 251*, 5352–5360.
Stern, A., Sedgwick, B., & Smith, S. (1982) *J. Biol. Chem. 257*, 799–803.
Stoops, J. K., & Wakil, S. J. (1981) *J. Biol. Chem. 256*, 5128–5133.
Yun, S., & Hsu, R. Y. (1972) *J. Biol. Chem. 247*, 2689–2698.

Purification and Characterization of a Calcium-Dependent Protease from Rat Liver†

George N. DeMartino* and Dorothy E. Croall

ABSTRACT: A calcium-dependent protease, previously identified in rat liver and designated peak II [DeMartino, G. N. (1981) *Arch. Biochem. Biophys. 211*, 253–257], was purified and characterized. The calcium-dependent proteolytic activity was accounted for by an 80 000-dalton protein. Depending on the method of purification, we found that this protease could be associated with a 28 000-dalton subunit, which was devoid of protease activity. The catalytic characteristics of the two different forms of the protease were indistinguishable. Each was half-maximally activated by approximately 250 μM calcium.

Calcium-dependent proteases have been identified in a number of tissues of various species (Murachi et al., 1981; Ishiura, 1981). In most cases, the structure of these enzymes appears to be a heterodimer with subunit molecular weights of 80 000 and 30 000 (Dayton et al., 1981; Mellgren et al., 1982; Hathaway et al., 1982). Some reports, however, describe the enzyme as a monomer of molecular weight approximately 80 000 (Kubota et al., 1981; Ishiura et al., 1978; Suzuki et al., 1981; Croall & DeMartino, 1983). Although in some instances these discrepancies may result from tissue and/or species-specific differences, in other cases the discrepancies exist for enzymes from a single source (Azanza et al., 1979; Tsuji & Imahori, 1981; Mellgren et al., 1982).

Recently, we identified two calcium-dependent proteases in rat liver (DeMartino, 1981). The purpose of the present work was to purify and characterize one of these enzymes, the form which requires high calcium concentrations and is designated peak II. In the course of these studies, we discovered that the subunit composition of the isolated enzyme was critically dependent on the method of purification. These results may provide insight into the reported differences for the protein composition of other calcium-dependent proteases.

Materials and Methods

Preparation of Calcium-Dependent Protease Peak II from Rat Liver. Partially purified calcium-dependent protease peak II was prepared through the diethylaminoethylcellulose (DEAE-cellulose)[1] ion-exchange chromatography step as previously described (DeMartino, 1981). In preparation for the affinity chromatography described below, the activity was dialyzed against 10 mM Tris-HCl, pH 7.5, 0.5 mM dithiothreitol (DTT), 400 mM KCl, and 0.1 mM EGTA.

Casein–Sepharose Affinity Chromatography of Calcium-Dependent Protease. Casein–Sepharose (15 g, approximately 50 mL of packed gel) was washed and equilibrated with 10 mM Tris-HCl, pH 7.5, 0.5 mM DTT, 400 mM KCl, and 1 mM $CaCl_2$. In order to minimize the time that the protease would spend in the presence of calcium but without substrate, the sample was applied to the column in a batchwise procedure. That is, 50% of the casein–Sepharose was placed in a beaker, and 50% was packed in a 2.5-cm diameter column. To activate the protease, a small volume of 1 M $CaCl_2$ was added to the dialyzed enzyme to achieve a final concentration of 1 mM $CaCl_2$, and this was immediately mixed with the casein–Sepharose in the beaker. This slurry was then applied to the rest of the casein–Sepharose packed in the column. The resin was washed extensively in the buffer described above. The bound protease was eluted in 10 mM Tris-HCl, pH 7.5, 0.5 mM DTT, 400 mM KCl, and 5 mM EGTA. Except where noted, this and all other procedures were carried out at 0–4 °C.

Preparation of Casein–Sepharose 4B. α-Casein (Sigma) was coupled to cyanogen bromide activated Sepharose 4B

† From the Department of Physiology, University of Texas Health Science Center, Dallas, Texas 75235. *Received April 29, 1983.* This work was supported by grants from the National Institutes of Health (AM-29829), the Muscular Dystrophy Association, and the American Heart Association.

[1] Abbreviations: DEAE, diethylaminoethyl; DTT, dithiothreitol; EGTA, ethylene glycol bis(β-aminoethyl ether)-*N,N,N',N'*-tetraacetic acid; SDS, sodium dodecyl sulfate; PAGE, polyacrylamide gel electrophoresis; Tris, tris(hydroxymethyl)aminomethane; EDTA, ethylenediaminetetraacetic acid.

0006-2960/83/0422-6287$01.50/0